ChemComm

Accepted Manuscript

This article can be cited before page numbers have been issued, to do this please use: B. Qiu, Q. Zhu, M. Xing and J. Zhang, *Chem. Commun.*, 2016, DOI: 10.1039/C6CC08311K.

View Article Online
DOI: 10.1039/C6CC08311K

Journal Name

COMMUNICATION

A robust and efficient catalyst of $Cd_xZn_{1-x}Se$ motivated by the CoP for the photocatalytic hydrogen evolution under the sunlight irradiation

Received 00th January 20xx,
Accepted 00th January 20xx

DOI: 10.1039/x0xx00000x

www.rsc.org/

Bocheng Qiu,[a] Qiaohong Zhu,[a] Mingyang Xing*[a] and Jinlong Zhang*[a]

$Cd_xZn_{1-x}Se$/CoP composites have been well studied as an effervescent photocatalyst for the H_2 evolution, which have a high efficiency of 45.1 mmol/h^{-1}·g^{-1}, a high quantum yield of 11.8% at ~520 nm. The tunable energy band of $Cd_xZn_{1-x}Se$ facilitates the photo-electrons transferring to CoP by the chemical bonds between the components. The advances in $Cd_xZn_{1-x}Se$/CoP for the photocatalytic H_2 evolution provide a new strategy for the splitting of seawater in the future.

Hydrogen is widely considered as one of the most promising green energy to replace the fossil fuel in the near future.[1-4] However, the most effective catalytic hydrogen production technology is the electrocatalytic water reduction,[5, 6] and the photocatalytic water reduction is still in the exploratory stage, owing to its too low hydrogen production which is very far away from the requirements of application. Compared with electrocatalysis, photocatalysis is an extremely green technology and its process is much simpler and lower cost. Until now, most of the reports on the photocatalysis-driven H_2 production are focusing on a relative value, which is always amplified by multiplying the mass of the catalyst.[7-9] That is why less reports can observe the effervescent hydrogen bubbles on the catalyst surface under the outdoor sunlight irradiation, even though the relative hydrogen evolution rate has been much higher than 0.2 mmol•g^{-1}•h^{-1} [10, 11]

Moreover, the noble metals are considered as the best cocatalysts for the photocatalytic H_2 evolution,[1] but the high cost greatly limits their practical values. Hence, it is an incontrovertible fact that exploring the highly efficient and noble-metal-free cocatalysts in water splitting is still the hotspot in the future photocatalysis research. Although many efficient cocatalysts based on earth abundant metals such as Mo,[12, 13] Co,[9, 14] and Ni,[4, 15] have been developed in the photocatalytic H_2 evolution, their absolute value of H_2 production quantity is still too low, which is not strong enough to produce a large number of eyeable hydrogen bubbles directly under the outdoor sunlight irradiation, especially when the catalyst is exposed to the air to split the seawater. Additionally, the mechanism of the enhanced hydrogen evolution rate induced by the cocatalysts is still unclear, and we always puzzled that not all the semiconductors can fit the same cocatalyst. The fabrication of catalyst with tunable energy band is expected to explain this phenomena.

Herein, the photocatalyst of $Cd_xZn_{1-x}Se$ nanotubes with a tunable energy band was successfully fabricated by an ion exchange method, which can be motivated by the CoP nanoparticles to produce effervescent and eyeable H_2 bubbles in the outdoor sunlight irradiation. The absolute value of H_2 production quantity of 50 mg $Cd_{0.25}Zn_{0.75}Se$/CoP under the visible light (>420 nm) irradiation can be up to 1.2 mmol· h^{-1}, and its quantum efficiency at the wavelength of 520 nm is up to 11.8%. The achievement of the tunable energy band of $Cd_xZn_{1-x}Se$ by changing the concentration of Cd is hoping to help us to understand the electron transfer between $Cd_xZn_{1-x}Se$ and CoP.

Firstly, ZnSe-DETA (DETA=diethylenetriamine) nanobelts were synthesized by a hydrothermal method according to the reported literatures,[16, 17] as shown in Fig. S1 and S2. The Cd element was successfully introduced into the ZnSe-DETA to obtain the $Cd_xZn_{1-x}Se$ nanotubes by partial substitution of Zn via a simple ion-exchange method (x represents the concentration of Cd, x = 0.25, 0.5, 0.75 and 1.0). Inductively coupled plasma emission spectrograph (ICP) was used to confirm the molar ratio of Cd^{2+} to Zn^{2+} (Table S1). It is noted that the DETA molecules can be dissolved in the ion-exchange process.[18] Interestingly, the introduction of Cd causes the nanobelts to be hollow structure with a thinner middle (TEM and SEM images in Fig. S3), which is consistent with the reported literature.[17] The nanotubes are formed through coupled processes such as the Kirkendall effect, the dissolution of ZnSe-DETA nanobelts, recrystallization, oriented attachment

---

[a] *Key Laboratory for Advanced Materials and Institute of Fine Chemicals, School of Chemistry and Molecular Engineering, East China University of Science and Technology, 130 Meilong Road, Shanghai 200237, P.R. China. E-mail: mingyangxing@ecust.edu.cn, jlzhang@ecust.edu.cn*

Electronic Supplementary Information (ESI) available: Experimental details and additional Fig.s are provided including TEM, XRD, UV-DRS, nitrogenadsorption–desorption isotherms, XPS, EIS Nyquist plots, and Mott–Schottky tests. See DOI: 10.1039/x0xx00000x

View Article Online
DOI: 10.1039/C6CC08311K

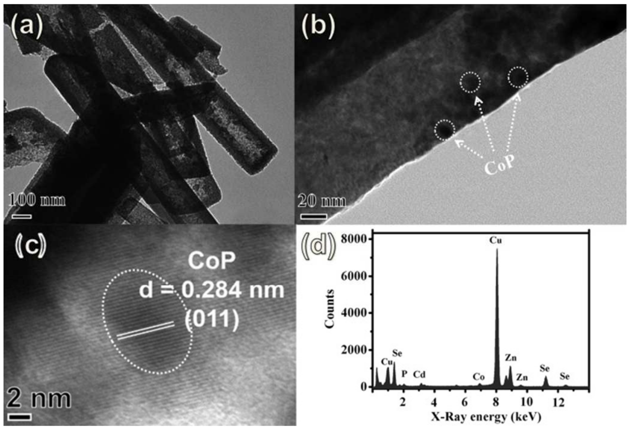

Fig. 1 (a, b) TEM and (c) HRTEM images for $Cd_{0.25}Zn_{0.75}Se$/CoP (amplification for the white cycle in (b)). (d) EDX spectrum of $Cd_{0.25}Zn_{0.75}Se$/CoP (analysis of the region in (a))

of CdSe nanoparticles, and an Ostawald ripening process.[17] The as-prepared $Cd_xZn_{1-x}Se$ nanotubes consist of nanoparticles assembled along the [001] direction (Fig. S3d). The XRD results also indicate that the fully CdSe would be generated with the increase of Cd concentration (Fig. S4).

On the other hand, CoP nanoparticles were successfully synthesized through a CVD-like method by using $Co(OH)_2$ and NaH_2PO_2 as the precursors (Fig. S5). The major diffraction peaks in the XRD spectrum can be indexed to the diffraction from the characteristic planes of orthorhombic CoP (Fig. S6).[19] The compounding of $Cd_xZn_{1-x}Se$ nanotubes and CoP nanoparticles were achieved via a simple mechanical mixing method. TEM image (Fig. 1a) shows that $Cd_{0.25}Zn_{0.75}Se$/CoP has an average diameter of 200 nm, length of 0.5-3 μm and high surface area of ~108.5 m^2/g from BET (Fig. S7). There is no remarkable morphology change when the loading ratio of CoP is increasing (Fig. S8). Besides, TEM image displays that some CoP nanoparticles (white circles in Fig. 1b) have been loaded on the wall of $Cd_xZn_{1-x}Se$ nanotubes rather than in the form of free particles, which implies some chemical bonds are generated during the mixing process. The HRTEM image (Fig. 1c) gives the characteristic lattice fringes of (011) facets in CoP, also indicating the CoP nanoparticles are successfully loaded on the walls of $Cd_xZn_{1-x}Se$. Moreover, the Energy-dispersive X-ray spectrum (EDX; Fig. 1d) further confirms the formation of $Cd_{0.25}Zn_{0.75}Se$/CoP with Cd, Zn, Se, Co and P as the principal elemental components (Cu peak emanate from the carbon-coated TEM grid).

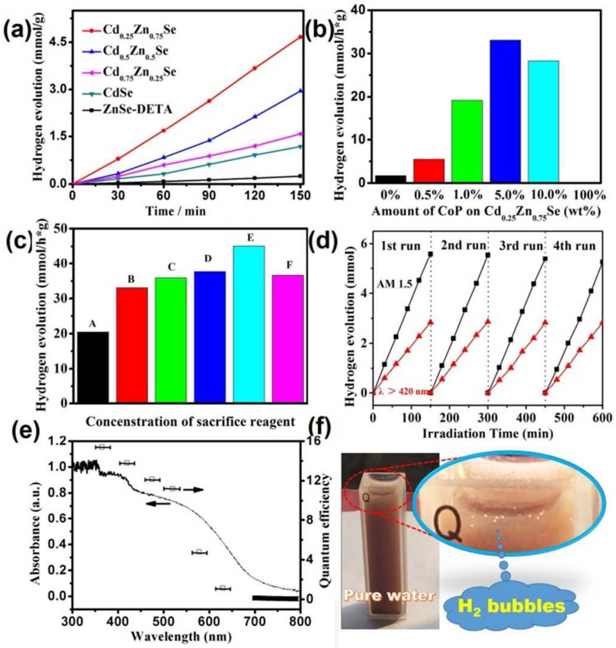

Fig. 2 (a) Photocatalytic H_2 evolution over different catalysts in the absence of CoP under the simulated solar light irradiation (300 W Xe lamp with AM 1.5 filter; 0.50 M Na_2S, 0.50 M Na_2SO_3); (b) Photocatalytic H_2 evolution on $Cd_{0.25}Zn_{0.75}Se$ loaded with different amount of CoP (300 W Xe lamp with AM 1.5 filter; 0.50 M Na_2S, 0.50 M Na_2SO_3); (c) Photocatalytic H_2 evolution on $Cd_{0.25}Zn_{0.75}Se$ loaded with 5.0 wt% CoP in the presence of different concentration of sacrificial reagents (300 W Xe lamp with AM 1.5 filter; A: 0.25 M Na_2S, 0.35 M Na_2SO_3; B: 0.50 M Na_2S, 0.50 M Na_2SO_3; C: 0.75 M Na_2S, 1.25 M Na_2SO_3; D: 1.00 M Na_2S, 1.40 M Na_2SO_3; E: 1.25 M Na_2S, 1.75 M Na_2SO_3; F: 1.50 M Na_2S, 2.10 M Na_2SO_3); (d) The absolute values of H_2 production quantity over $Cd_{0.25}Zn_{0.75}Se$/CoP (50 mg catalyst loaded with 5.0 wt% CoP in 100 mL aqueous solution containing 1.25 M Na_2S and 1.75 M Na_2SO_3; light source: 300 W Xe lamp with AM 1.5 filter and visible light with λ > 420 nm); (e) Quantum yield of H_2 evolution at different wavelengths by using the catalyst of $Cd_{0.25}Zn_{0.75}Se$/CoP (irradiated by a 300 W Xe lamp using a bandpass filter of λ ± 20 nm for 365, 420, 475, 520, 578, 630 nm; and a longpass cutoff filter for λ > 700 nm); (f) The picture of H_2 evolution over the $Cd_{0.25}Zn_{0.75}Se$/CoP under the outdoor sunlight irradiation (3.0 mg catalyst loaded with 5.0 wt% CoP in 3.0 mL aqueous solution containing 1.25 M Na_2S and 1.75 M Na_2SO_3).

The XPS data of $Cd_{0.25}Zn_{0.75}Se$/CoP was collected to investigate the interaction between the main semiconductors and CoP. The XPS full spectra further confirm the element formation of $Cd_{0.25}Zn_{0.75}Se$/CoP and $Cd_{0.25}Zn_{0.75}Se$ (Fig. S9). The disappearing of the peak at 778.7 eV of reduced Co in the Co2p XPS spectrum after the compounding of $Cd_{0.25}Zn_{0.75}Se$ suggests the occurring of oxidation reaction at the interface between $Cd_{0.25}Zn_{0.75}Se$ and CoP (Fig. S10a).[20, 21] It is well known that the pure CoP is easy to be oxidized by the oxygen in the air and produce the peak at 781.8 and 134.6 eV in the Co2p and P2p XPS spectra (Fig. S10a,b),[21, 22] respectively. Interestingly, after mechanical mixing with $Cd_{0.25}Zn_{0.75}Se$, the oxidation peak at 134.6 eV has shifted to a lower binding energy of 133.5 eV, which means too many charges are transferring from Co to P.[22] It is very similar to the hydrogenases and metal complex catalysts, the surface of CoP also features pendant base P (δ^-) moieties in close proximity to the metal center Co (δ^+).[22] From Fig. S10c, the Se 3d peak at 52.6 eV in $Cd_{0.25}Zn_{0.75}Se$ shifted to a lower binding energy of 52.3 eV after compositing with CoP. It can be deduced that

View Article Online
DOI: 10.1039/C6CC08311K

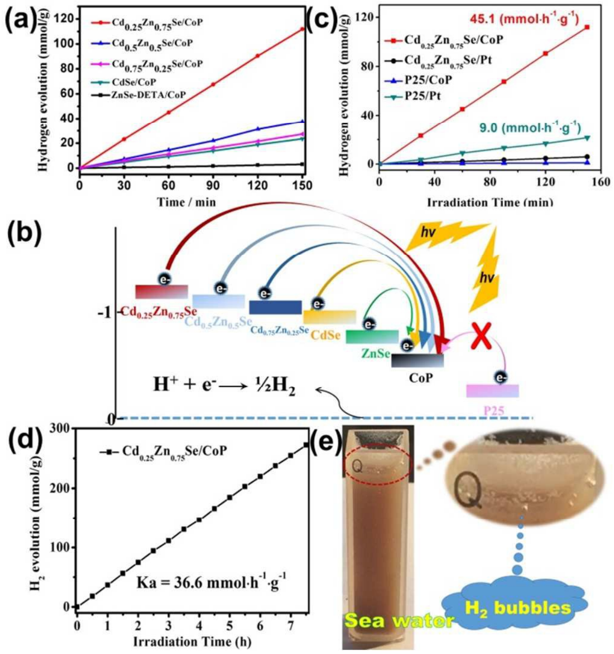

Fig. 3 (a) Photocatalytic H_2 evolution over different catalysts loaded with 5 wt% CoP under the simulated solar light irradiation (1.25 M Na_2S, 1.75 M Na_2SO_3); (b) Structural model of the energy states for different catalysts; (c) H_2 production comparison by using different co-catalysts; (d) Photocatalytic H_2 evolution over the $Cd_{0.25}Zn_{0.75}Se$/CoP under the simulated solar light irradiation; (e) The picture of H_2 evolution in the artificial seawater system over the $Cd_{0.25}Zn_{0.75}Se$/CoP under the outdoor sunlight irradiation.

part of Se oxidized the reduced Co to form the Co-Se bond. The Co-Se bond between $Cd_{0.25}Zn_{0.75}Se$ and CoP would improve the charge transfer from Co to P (δ^-) while at the same time it would decrease the reduced Co (δ^+) and increase the electron density in the active sites of P (δ^-) for improved acceptance of protons. In addition, we investigated the contact interfaces between $Cd_{0.25}Zn_{0.75}Se$ and CoP through HRTEM to confirm the existence of Co-Se bond. As shown in Fig. S11, there existed an obvious closed contact interface, which revealed existing possibility of Co-Se bond. In order to further confirm the interaction between the main semiconductors and CoP, we prepared P25/CoP composite (Fig. S12) and used XPS spectra to investigate it (Fig. S13). Similar to $Cd_{0.25}Zn_{0.75}Se$, P25 also should produce oxidation bond with CoP when they are mixed together in the air. Compared with the UV-DRS spectrum of $Cd_{0.25}Zn_{0.75}Se$, the absorption shoulder of $Cd_{0.25}Zn_{0.75}Se$/CoP has a significant red-shift, as shown in Fig. S14a, which indicates the chemical connection between $Cd_{0.25}Zn_{0.75}Se$ and CoP rather than a physical mixing process. The dramatically enhanced photo-current intensity of $Cd_{0.25}Zn_{0.75}Se$ after loading of CoP also reveals the efficient transfer of photo-electrons from $Cd_{0.25}Zn_{0.75}Se$ to CoP by some chemical bonds (Fig. S14b), as evidenced by the reduced charge transfer resistance (Fig. S15).

In order to obtain the optimal photocatalytic condition for the hydrogen evolution under the solar light irradiation, the Cd concentration in $Cd_xZn_{1-x}Se$, the CoP loading amount in composite, and the dosage of the sacrificial reagents are all investigated in Fig. 2. The photocatalytic activities of $Cd_xZn_{1-x}Se$ in the absence CoP are shown in Fig. 2a. With the increasement of Cd concentration, the H_2 production increases firstly and then decreases. The $Cd_{0.25}Zn_{0.75}Se$ has the highest photocatalytic activity for the H_2 evolution, owing to that a proper Cd concentration would lead to a high location of conduction band (CB) with a strong electron reduction ability. This result is in good accordance with that of photocurrent (Fig. S14b). The next step was to use the $Cd_{0.25}Zn_{0.75}Se$ as the main semiconductor and investigate the influence of the loading amount of CoP on the H_2 production. Seen from Fig. 2b, when the weight ratio of CoP is 5.0 %, the composite displays the highest photocatalytic H_2 production. The last is to determine the optimal dosage of sacrificial reagents. When the 1.25 M Na_2S and 1.75 M Na_2SO_3 are employed as the sacrificial reagents in the solution, the $Cd_{0.25}Zn_{0.75}Se$/CoP (5.0%) presents the best H_2 evolution (Fig. 2c). Thereby, the optimal photocatalytic system contains 50 mg $Cd_{0.25}Zn_{0.75}Se$/CoP (5.0%) in 100 mL aqueous solution containing 1.25 M Na_2S and 1.75 M Na_2SO_3 as sacrificial reagents.

The absolute values of H_2 production quantity of 50 mg $Cd_{0.25}Zn_{0.75}Se$/CoP (5.0%) under the simulated solar light (AM 1.5 filter) and visible light (λ>420 nm) are shown in Fig. 2d. It is approximatively 2.3 mmol·h^{-1} and 1.2 mmol·h^{-1} H_2 are produced in the solar light and visible light irradiation, respectively. The $Cd_{0.25}Zn_{0.75}Se$/CoP exhibits substantial activity and stability in the context of photocatalytic production of H_2 under light irradiation. Even after 4 times cycles, it still remains stable and high photocatalytic H_2 production. Most importantly, the quantum efficiency can be up to 13.8 % at ~420 nm and 11.8 % even at ~520 nm (Fig. 2e), which implies it can sufficiently release eyeable H_2 bubbles under the outdoor sunlight irradiation. Hence, 3.0 mg catalysts was exposed to the air and directly illuminated by the sunlight, as shown in Fig. 2f. Many macroscopic bubbles with a radius of ~1.0 mm were continuously released over the $Cd_{0.25}Zn_{0.75}Se$/CoP catalysts (details are shown in the Movie S1). Interestingly, if the dosage of the catalysts was increased to 200 or 500 mg, some larger H_2 bubbles can also be released by the $Cd_{0.25}Zn_{0.75}Se$/CoP under the simulated solar light irradiation (Movie S2). With the increasing of catalyst dosage, the radius and speed of H_2 bubbles also increase significantly, which indicates the H_2 evolution efficiency is direct proportion to the amount of catalyst.

For the investigation of photocatalytic mechanism of $Cd_xZn_{1-x}Se$/CoP, the “Binding Matching” principle is the first essential which we should consider in the H_2 evolution. The bandgaps and CB of different semiconductors are calculated by the Kubelka-Munk function (Fig. S16) and Mott-schottky curves (Fig. S17), respectively, which are summarized in Table S2. The CoP nanoparticles are not stable enough under the light irradiation, owing to the reduction of Co and the rising of the valence band (VB, shifting from 0.050 eV to -0.420 eV), as shown in Fig. S18 and S19. After the irradiation, its VB position of CoP is higher than the hydrogen production energy level.

View Article Online
DOI: 10.1039/C6CC08311K

Thereby, we can eliminate that the photo-electrons for the H_2 evolution is coming from the CoP. The photocatalytic activities for the H_2 evolution over different semiconductors with 5.0 wt% CoP were carried out in the aqueous solution containing optimal sacrificial reagents, and the results are shown in Fig. 3a. Seen from Table 1 and Fig. 3a, the bandgaps and CBs of $Cd_xZn_{1-x}Se$ can be tunable by changing the Cd concentration, and the photocatalytic H_2 evolution activity is increase with the decrease of the CB values of $Cd_xZn_{1-x}Se$, which completely conforms to the “Band Matching” theory for the H_2 evolution. That is, the electrons on higher location of CB in $Cd_xZn_{1-x}Se$ has a better transfer efficiency to CoP and reduction capacity for the H_2 production, as shown in Fig. 3b. Although P25 has a good charge transfer efficiency to Pt, it cannot transfer the photo-electrons to CoP due to its lower location of CB than that of CoP (Table S1). That is why the photocatalytic activity of P25/CoP is much lower than that of P25/Pt (Fig. 3c).

In addition to the energy matching between $Cd_xZn_{1-x}Se$ and CoP, the ability to capture the protons of CoP itself is another very important role in enhancing the photocatalytic H_2 evolution. As above mentioned in the XPS discussion, some oxidation bonds generated between $Cd_xZn_{1-x}Se$ and CoP would facilitate the acceptance of protons. Hence, compared with the traditional cocatalysts of Pt (the TEM images of $Cd_{0.25}Zn_{0.75}Se$/Pt are shown in Fig. S20). CoP is not only very cheap but also good at adsorption of protons and facilitation of H_2 evolution.[21, 22] P25/Pt is widely considered as one of the most efficient photocatalysts for the H_2 evolution when using methanol as the sacrificial reagent.[23] For comparison, we prepared P25/Pt through the photodeposition method (Fig. S21). Unfortunately, it still cannot release eyeable H_2 bubbles no matter under the Xe lamp irradiation or sunlight irradiation. It is an incontrovertible fact that the $Cd_{0.25}Zn_{0.75}Se$/CoP displays a much higher H_2 production efficiency than the P25/Pt (its “Ka” is 5 times larger than that of P25/Pt, seen from Fig. 3c).

Except for photocatalytic water splitting, we also have done the photocatalytic splitting on artificial seawater to highlight the catalysts of $Cd_{0.25}Zn_{0.75}Se$/CoP having a large practical application value, as shown in Fig. 3d,e. Under the simulated solar light irradiation, the $Cd_{0.25}Zn_{0.75}Se$/CoP has a high and stable H_2 production. Even after more than 7 hours irradiation, it still displays stable and linear increasing trend, and the speed constant is keeping at 36.6 $mmol \cdot h^{-1} \cdot g^{-1}$ (Fig. 3d). Most importantly, the as-prepared catalysts also can photo-decompose seawater to release the continuous H_2 bubbles directly under the outdoor sunlight irradiation, as shown in Fig. 3e and Movie S3.

In conclusion, we employed a simple mechanical mixing method to successfully compound the $Cd_xZn_{1-x}Se$ nanotubes and CoP nanoparticles. The tunability of the energy band of $Cd_xZn_{1-x}Se$ was realized by changing the Cd concentration, which contributes to the acceptance of photo-electrons on the CoP nanoparticles. The electrons coming from the higher CB always have a stronger reduction capacity for the H_2 evolution. The $Cd_xZn_{1-x}Se$/CoP series catalysts with an excellent photocatalytic quantum efficiency display a large potential application for replacing the noble metals based materials in the seawater splitting.

This work has been supported by National Nature Science Foundation of China (21577036, 21377038, 21237003 and 21677048), the Science and Technology Commission of Shanghai(16JC1401400) and sponsored by “Chenguang Program” supported by Shanghai Education Development Foundation and Shanghai Municipal Education Commission (14CG30), and the Fundamental Research Funds for the Central Universities (22A201514021).

Notes and references

1 Q. Wang, T. Hisatomi, Q. Jia, H. Tokudome, M. Zhong, C. Wang, Z. Pan, T. Takata, M. Nakabayashi, N. Shibata, Y. Li, I. D. Sharp, A. Kudo, T. Yamada and K. Domen, *Nat. Mater*, 2016, **15**, *611-615*.
2 S. Cao, Y. Chen, C.-J. Wang, X.-J. Lv and W.-F. Fu, *Chem. Commun.*, 2015, **51**, 8708-8711.
3 S. Cao, Y. Chen, C.-J. Wang, P. He and W.-F. Fu, *Chem. Commun.*, 2014, **50**, 10427-10429.
4 Z. Sun, H. Zheng, J. Li and P. Du, *Energ. Environ. Sci.*, 2015, **8**, 2668-2676.
5 L. Yu, B. Y. Xia, X. Wang and X. W. Lou, *Adv. Mater.*, 2016, **28**, 92-97.
6 P. Zhang, M. Wang, Y. Yang, T. Yao, H. Han and L. Sun, *Nano Energy*, 2016, **19**, 98-107.
7 X. Chen, L. Liu, P. Y. Yu and S. S. Mao, *Science*, 2011, **331**, 746-750.
8 T. Simon, N. Bouchonville, M. J. Berr, A. Vaneski, A. Adrović, D. Volbers, R. Wyrwich, M. Döblinger, A. S. Susha, A. L. Rogach, F. Jäckel, J. K. Stolarczyk and J. Feldmann, *Nat. Mater.*, 2014, **13**, 1013-1018.
9 L. Liao, Q. Zhang, Z. Su, Z. Zhao, Y. Wang, Y. Li, X. Lu, D. Wei, G. Feng, Q. Yu, X. Cai, J. Zhao, Z. Ren, H. Fang, F. Robles-Hernandez, S. Baldelli and J. Bao, *Nat. Nanotechnol.*, 2014, **9**, 69-73.
10 X. Chen, L. Liu, Y. Y. Peter and S. S. Mao, *Science*, 2011, **331**, 746-750.
11 J. Liu, Y. Liu, N. Liu, Y. Han, X. Zhang, H. Huang, Y. Lifshitz, S.-T. Lee, J. Zhong and Z. Kang, *Science*, 2015, **347**, 970-974.
12 Q. Xiang, J. Yu and M. Jaroniec, *J. Am. Chem. Soc.*, 2012, **134**, 6575-6578.
13 G. Ye, Y. Gong, J. Lin, B. Li, Y. He, S. T. Pantelides, W. Zhou, R. Vajtai and P. M. Ajayan, *Nano Letters*, 2016, **16**, 1097-1103.
14 S. Chen, S. Shen, G. Liu, Y. Qi, F. Zhang and C. Li, *Angew. Chem. Int. Ed.*, 2015, **54**, 3047-3051.
15 Y. Shi and B. Zhang, *Chem. Soc. Rev.*, 2016, **45**, 1529-1541.
16 W. Yao, S. H. Yu, X. Y. Huang, J. Jiang, L. Q. Zhao, L. Pan and J. Li, *Adv. Mater.*, 2005, **17**, 2799-2802.
17 M. Zhang, Y. Lu, J.-F. Chen, T.-K. Zhang, Y.-Y. Liu, Y. Yang, W.-T. Yao and S.-H. Yu, *Langmuir*, 2010, **26**, 12882-12889.
18 X. Wu, Y. Yu, Y. Liu, Y. Xu, C. Liu and B. Zhang, *Angew. Chem. Int. Ed.*, 2012, **51**, 3211-3215.
19 H. Yang, Y. Zhang, F. Hu and Q. Wang, *Nano Letters*, 2015, **15**, 7616-7620.
20 A. P. Grosvenor, S. D. Wik, R. G. Cavell and A. Mar, *Inorg. Chem.*, 2005, **44**, 8988-8998.
21 A. W. Burns, K. A. Layman, D. H. Bale and M. E. Bussell, *Appl. Catal. A: General*, 2008, **343**, 68-76.
22 P. Jiang, Q. Liu, C. Ge, W. Cui, Z. Pu, A. M. Asiri and X. Sun, *J. Mater. Chem. A*, 2014, **2**, 14634-14640.
23 M. Xing, J. Zhang, B. Qiu, B. Tian, M. Anpo and M. Che, *Small*, 2015, **11**, 1920–1929.